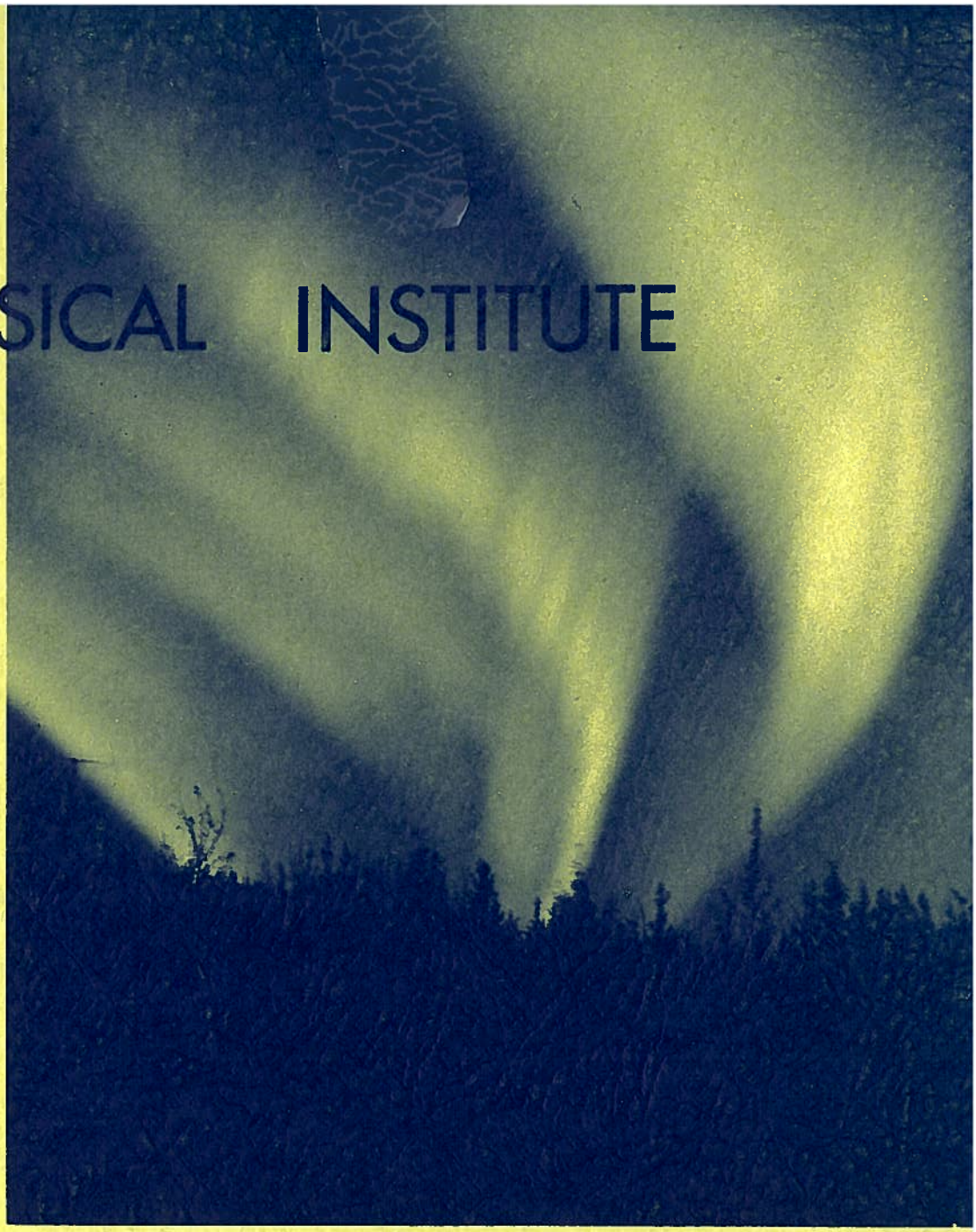

GEOPHYSICAL INSTITUTE

UNIVERSITY OF ALASKA

FAIRBANKS, ALASKA

UAG R-265

CHARGE-STATE-EQUILIBRATED H^+/H FLUX FRACTIONS FOR ANALYSIS OF THE HYDROGEN AURORA

by

Bert Van Zyl

Department of Physics
University of Denver

November 1978

CHARGE-STATE-EQUILIBRATED H^+/H FLUX FRACTIONS FOR ANALYSIS OF THE HYDROGEN AURORA

by

Bert Van Zyl
Department of Physics
University of Denver

November 1978

ACKNOWLEDGMENTS

This study was undertaken during a six weeks' visit at the Geophysical Institute of the University of Alaska made possible by support from the University of Denver, National Science Foundation Grant ATM76-80282, and the Geophysical Institute.

An (unpublished) compilation and tabulation of cross section data by Eugene Young of the University of Michigan (state affiliation) was helpful in the preparation of this report.

The author thanks J. Roger Sheridan and Manfred H. Rees of the Geophysical Institute for helpful discussions during this study.

Publication of this report has been made possible by the support of National Science Foundation Grant ATM76-17409 to the University of Alaska.

ABSTRACT

An analysis of the hydrogen aurora begins with a determination of the charge-state-equilibrium fractions of the proton/hydrogen atom flux traversing the atmosphere. Charge-exchange and ionization-stripping cross sections are compiled. Where no data exist, estimates of the required cross sections are made. Charge-state-equilibrium flux fractions are computed for N_2, O_2, and O targets. Net atmospheric charge-state-equilibrium flux fractions are then calculated as a function of altitude using the appropriate atmospheric constituent density ratios for these species.

I. INTRODUCTION

Since the discovery of hydrogen spectral line emissions in the aurora by Vegard[1] in 1939, the hydrogen aurora has been recognized as a separate phenomenon from the more dynamic displays that are caused by energetic electron fluxes. The diffuse hydrogen arc, which can occur separated from or overlapping an electron event, is attributed to the precipitation of energetic protons (H^+) into the high atmosphere.

The primary H^+ energy distribution has been reviewed by McNeal and Birely.[2] Although a wide range of energy distributions are found, many workers use a Maxwellian distribution,

$$\frac{dN}{dE} = AEe^{-E/\alpha} \quad , \qquad (1)$$

where E is the primary H^+ energy and dN/dE is the distribution function in the units protons per cm^2 sec ster keV. The parameter α is commonly called the e-folding energy and 2α represents the average H^+ energy for the distribution.

Typical nighttime proton events are generally attributed to H^+ showers with e-folding energies from about 5 to 50 keV.[3] On the other hand, the polar cusp aurora, which may be caused by the influx of solar-wind protons into the midday magnetic cleft, features H^+ energies in the 1 keV energy range.[4] Thus, any meaningful study of the hydrogen aurora must cover an energy range extending from below 100 eV to above 100 keV.

At energies above about 100 keV, the incident H^+ maintain their ionic identity and lose energy primarily by ionization of the neutral atmospheric gas. Below 100 keV, however, charge exchange reactions of the type

$$H^+ + M \longrightarrow H + M^+ \qquad (2)$$

become increasingly important, resulting in conversion of the H^+ flux into neutral hydrogen atoms. Fast H atoms are not magnetically confined and can move long distances at high altitudes before being reionized in subsequent collisions. This effect is responsible, in part, for the diffuse nature of the hydrogen aurora. At energies below about 100 keV, the effects of collisions of both H^+ and H with the atmospheric species must thus be included in an analysis of the hydrogen aurora.

The first step in such an analysis is the evaluation of the fraction of time the incident H^+ spend in the charged and in the neutral state as they move through the atmosphere. To first order, these fractions are given by

$$F_0 = \left(\frac{\sigma_{10}}{\sigma_{10} + \sigma_{01}} \right) \quad , \qquad F_1 = \left(\frac{\sigma_{01}}{\sigma_{10} + \sigma_{01}} \right) \qquad (3)$$

for neutrals (charge state 0) and ions (charge state 1), respectively. σ_{10} is the charge-exchange cross section (conversion from charge state 1 to 0), and σ_{01} is the reverse ionization-stripping cross section.[5]

The purpose of this report is to present values of the charge-state-equilibrium flux fractions F_1 and F_0 over the entire energy range of importance in the hydrogen aurora. Recent data for N_2 and O_2 targets, in particular for the σ_{01} cross sections, make this a worthwhile endeavor. Previous studies, such as the work of Allison,[6] could not treat the energy range below a few keV because of lack of cross section data. In addition, a crude attempt is made to estimate cross sections for atomic oxygen targets where no experimental data are available.

This report is not intended to be a critical review of all available cross section data of importance. However, where considerable disagreement (i.e., outside experimentally quoted uncertainties) exists between various sets of results, comments on the measurements will be made relative to the selection of the particular data used. Not all available results are included, and I apologize for the omission of some of the earlier studies. Not all data points for any specific set of measurements are shown in the various graphs. Finally, where investigators do not present individual data points (only depicting a curve showing the cross section shape), points are plotted at intervals sufficient to show the magnitude and energy dependence of the cross section curve presented.

II. THE CHARGE-EXCHANGE CROSS SECTIONS

The charge-exchange cross sections for H^+ on N_2, O_2, and O targets are presented in the form of graphs of cross section versus H^+ energy between 50 eV and 2500 keV.

a.) $H^+ + N_2$

The data compilation for the σ_{10} cross section for H^+ on N_2 is shown in Fig. 1. The line drawn through the various measured results is my estimate of a reasonable fit to the data presented. Most of the data points fall within $\pm$ 25% of the curve, this value being typical of many of the quoted experimental uncertainties.

At the lowest energies, however, the results of Gustafsson and Lindholm[7] and those of Monnom et al.[8] drop rapidly with decreasing energy, while the data of Koopman[9] suggest an upward inflection in the cross section. In my judgment, the energy dependence of the Gustafsson and Lindholm and Monnom et al. results show the expected trend.

The results of Koopman[9] were obtained by passage of a proton beam through a target gas cell containing parallel plates which, when electrically biased, were made to collect the slow N_2^+ ions formed. At the lower energies, however, these plates could also collect elastically-scattered protons, whose orbits through the target cell have been altered by the slow-ion collection field. Scattering through angles of less than 20° could cause such protons to arrive at the collector plates. Such angular scattering is not unreasonable considering this light projectile and heavy target combination. Since the number of such large-angle-scattered protons should increase roughly[18] as E^{-1}, the net effect would be a "slow ion" measurement falling increasingly above the true N_2^+ current with decreasing energy below a few hundred eV. The experimental arrangements employed by Gustafsson and Lindholm[7] and Monnom et al.[8] should be less sensitive to this problem.

In addition, there seems to be little physical reason for this cross section to have the upward inflection exhibited by the Koopman[9] data.

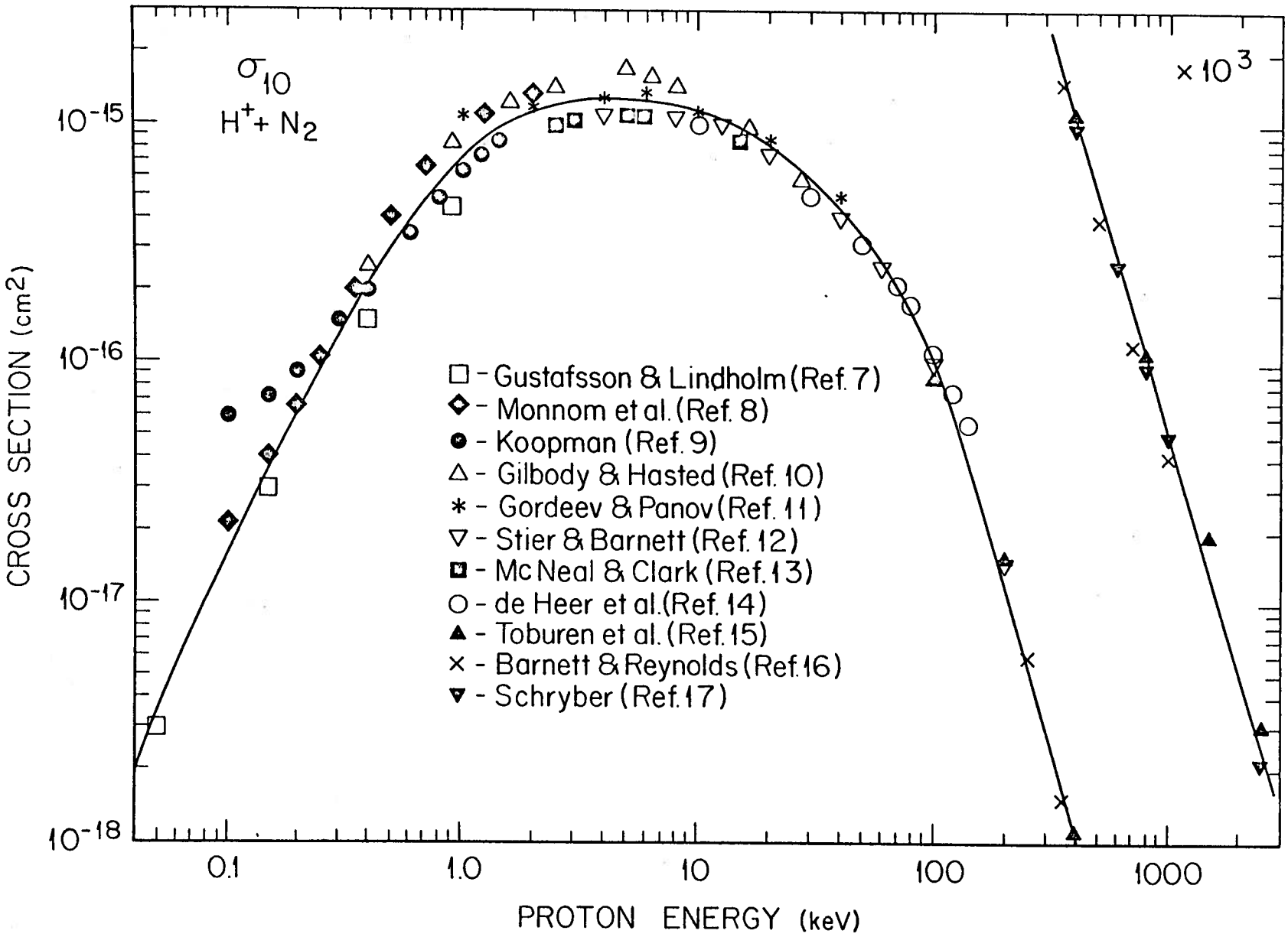

Figure 1. Charge-exchange cross section for protons in N_2.

Indeed, most such non-resonant (energy defect $\Delta E \gtrsim 2$ eV) charge exchange cross sections fall rapidly with decreasing energy in this energy range. The results of Gustafsson and Lindholm[7] and of Monnom et al.[8] show a cross section energy dependence close to E^2 (or v^4), a result which is consistent with the semiclassical theory of such collisions developed by Rapp and Francis.[19] Thus, the σ_{10} curve drawn in Fig. 1 is assumed to have the energy dependence of the Gustafsson and Lindholm and the Monnom et al. data.

b.) $H^+ + O_2$

The results for O_2 targets are shown in Fig. 2. In general, the agreement between the various measurements is satisfactory. Note that the near-resonant ($\Delta E < 1$ eV for many of the low-lying O_2^+ vibrational levels) nature of this reaction results in a large cross section to much lower energies than for N_2 targets. Again, the curve drawn through the various data points is adopted as a working cross section.

c.) $H^+ + O$

Cross section data for atomic oxygen targets are generally sparse. Fortunately, the charge-exchange cross section σ_{10} has been measured by Stebbings et al.[20] between 50 eV and 10 keV. This charge-exchange reaction is of the accidentally-resonant type ($\Delta E \gtrsim 0$) since the ionization potentials of both H and O are about 13.6 eV. The energy dependence of such cross sections for collision velocities below about 10^8 cm/sec (about 5 keV for proton impact) is typically given by

$$\sqrt{\sigma_{10}} = A - B(\log E), \qquad (4)$$

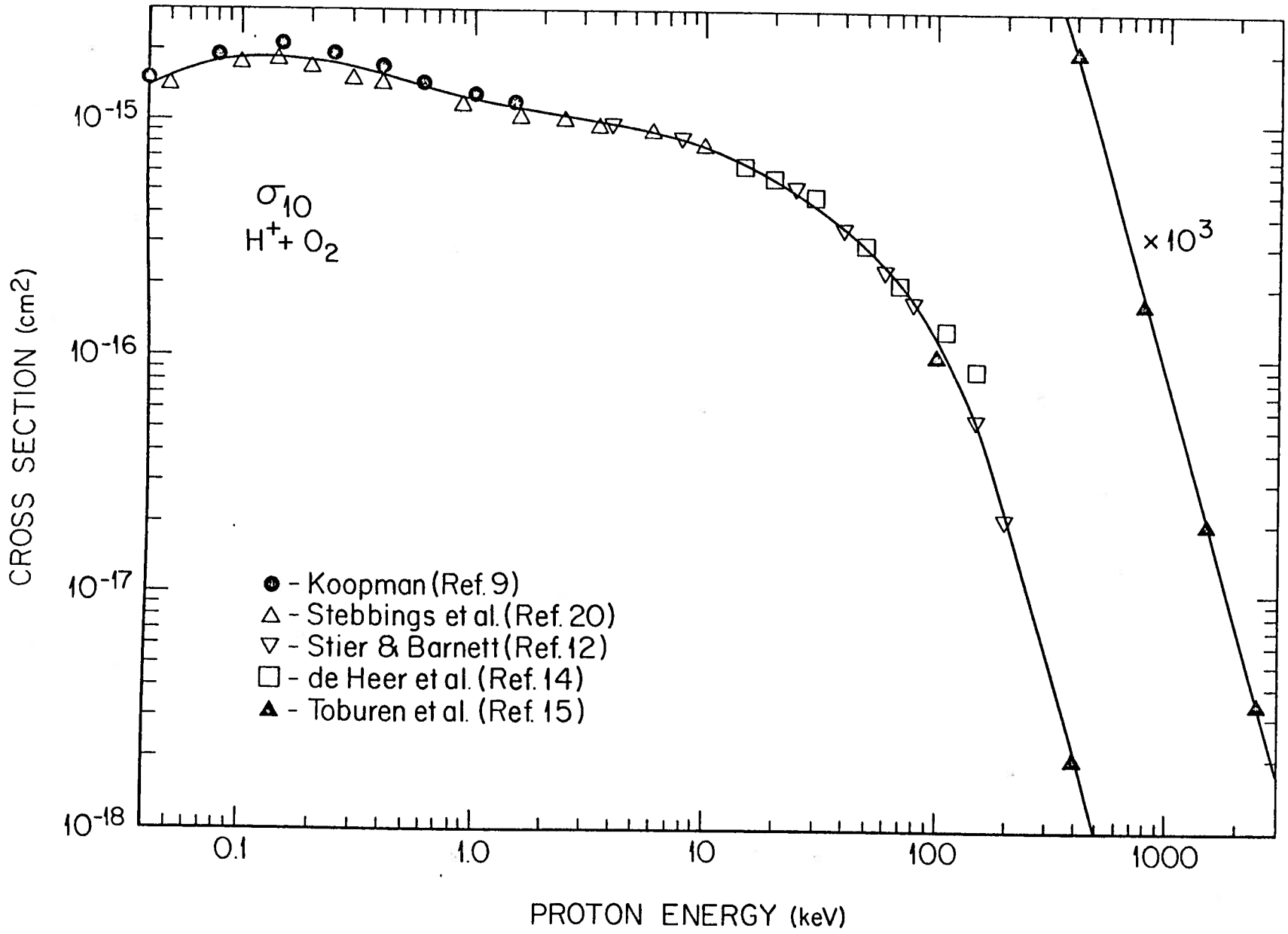

Figure 2. Charge-exchange cross section for protons in O_2.

where A and B are constants. At higher velocities, the charge-exchange cross section drops increasingly faster with energy due to the difficulty of delivering enough linear momentum to the exhanged electron to allow it to be captured by the passing proton.[21]

Fig. 3 shows the results of Stebbings et al.[20] (note that the square root of the cross section is plotted) and their fit to the form of Eq. 4. As can be seen, the fit is quite satisfactory out to about 5 keV. Also shown are the symmetric resonant cross section for the $H^+ + H$ reaction and the $H^+ + O_2$ charge-exchange cross section from Fig. 2. Note that both of these cross sections have energy dependences which begin to deviate from the "straight-line" form of Eq. 4 at about 5 keV proton energy and fall much more rapidly at the higher energies.

McNeal and Birely[2] have assumed that the σ_{10} cross section measured by Stebbings et al.[20] can be extrapolated into the higher energy region in accordance with the form of Eq. 4. Since neither the $H^+ + H$ or the $H^+ + O_2$ charge-exchange cross sections follow such an extrapolation, and the theory predicts that the cross section should drop off much more rapidly at the higher energies,[19,21] I find this extrapolation to be of questionable merit. I therefore use an extrapolation exhibiting an energy dependence similar to that found for the $H^+ + H$ and $H^+ + O_2$ charge-exchange cross sections, as shown by the solid line in Fig. 3. Indeed, the last few data points of Stebbings et al. appear to be consistent with such a prediction. My extrapolated data yield a value for $\sigma_{10}(O)$ of about $0.8\sigma_{10}(O_2)$ at energies above 20 keV. While the true shape of this cross section curve will have to await additional experimental measurements or theoretical calculations, it seems likely that the basic energy dependence will be roughly that of the crude estimate presented here.

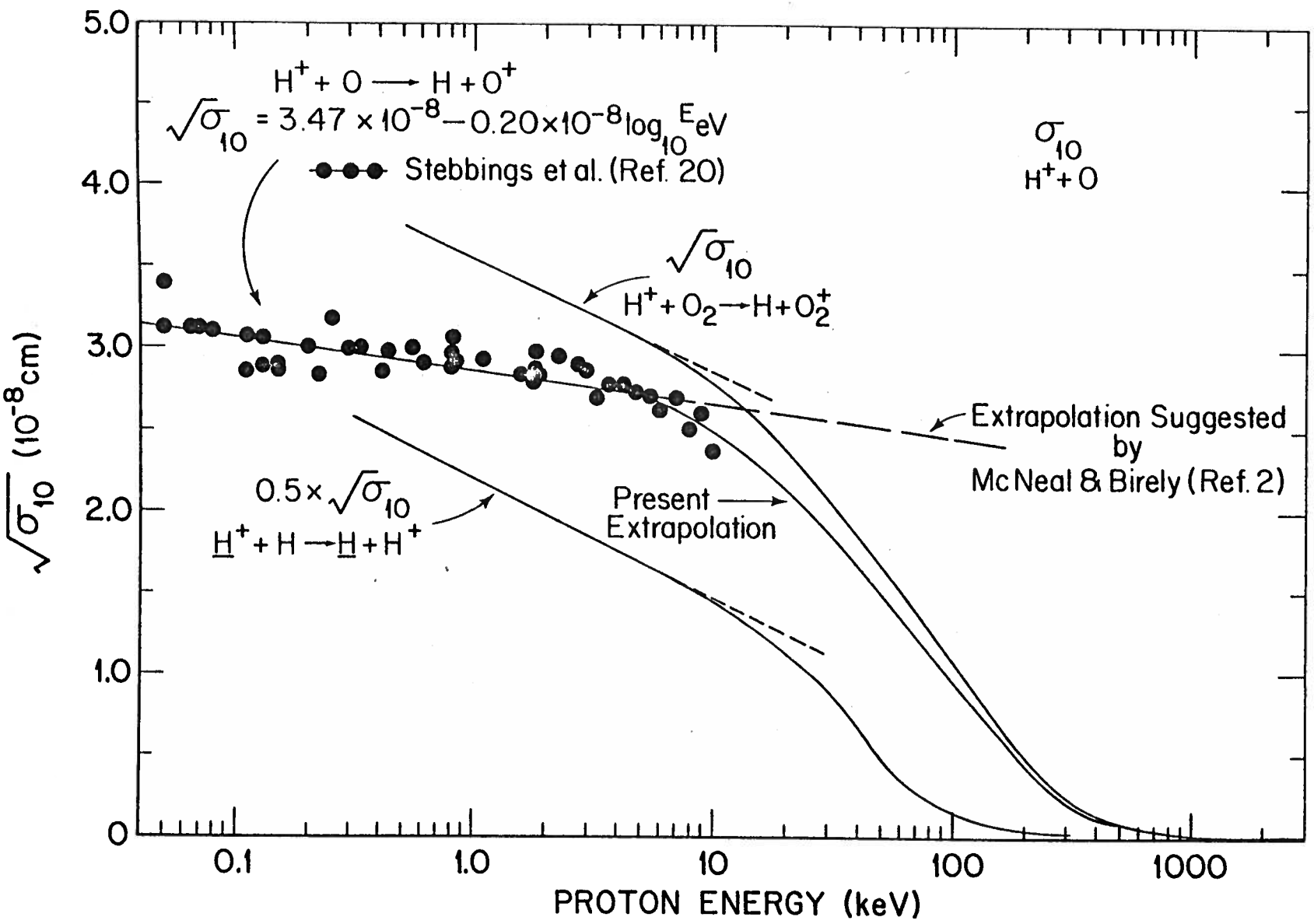

Figure 3. Charge-exchange cross section for protons in O. The charge-exchange cross sections for $H^+ + H$ and $H^+ + O_2$ are shown for comparison.

III. THE IONIZATION-STRIPPING CROSS SECTIONS

Results of the data compilation for the σ_{01} cross sections, i.e., reactions of the type

$$H + M \longrightarrow H^+ + e^- + M \quad , \qquad (5)$$

are again presented graphically over the same energy range as the charge-exchange cross sections discussed above.

a.) $H + N_2$

The data for N_2 targets are shown in Fig. 4. Despite the inherently more difficult nature of such experiments (in preparing and absolutely measuring the neutral atom beam intensity), the disagreement between the various sets of data is normally less than a factor of two. Where such disagreement exists, primarily in the 1 to 20 keV energy region, I feel that most of the older experiments have led to an underestimate of the true cross section. This results from experimental difficulties associated with secondary electron effects (released from surfaces inside the experimental apparatus) and angular scattering of the fast reaction-product protons allowing them to escape detection. Detailed discussions of how such problems can influence such measurements have been presented elsewhere[18,22] and will not be repeated here.

The more recent results of Van Zyl et al.,[22] Smith et al.,[23] and Cisneros et al.,[24] are in reasonable agreement between 0.5 and 5 keV, even though the experimental techniques employed for the measurements were very different. In my opinion, the 250 eV data point of Smith et al. is low because some of the protons produced in their experiment were

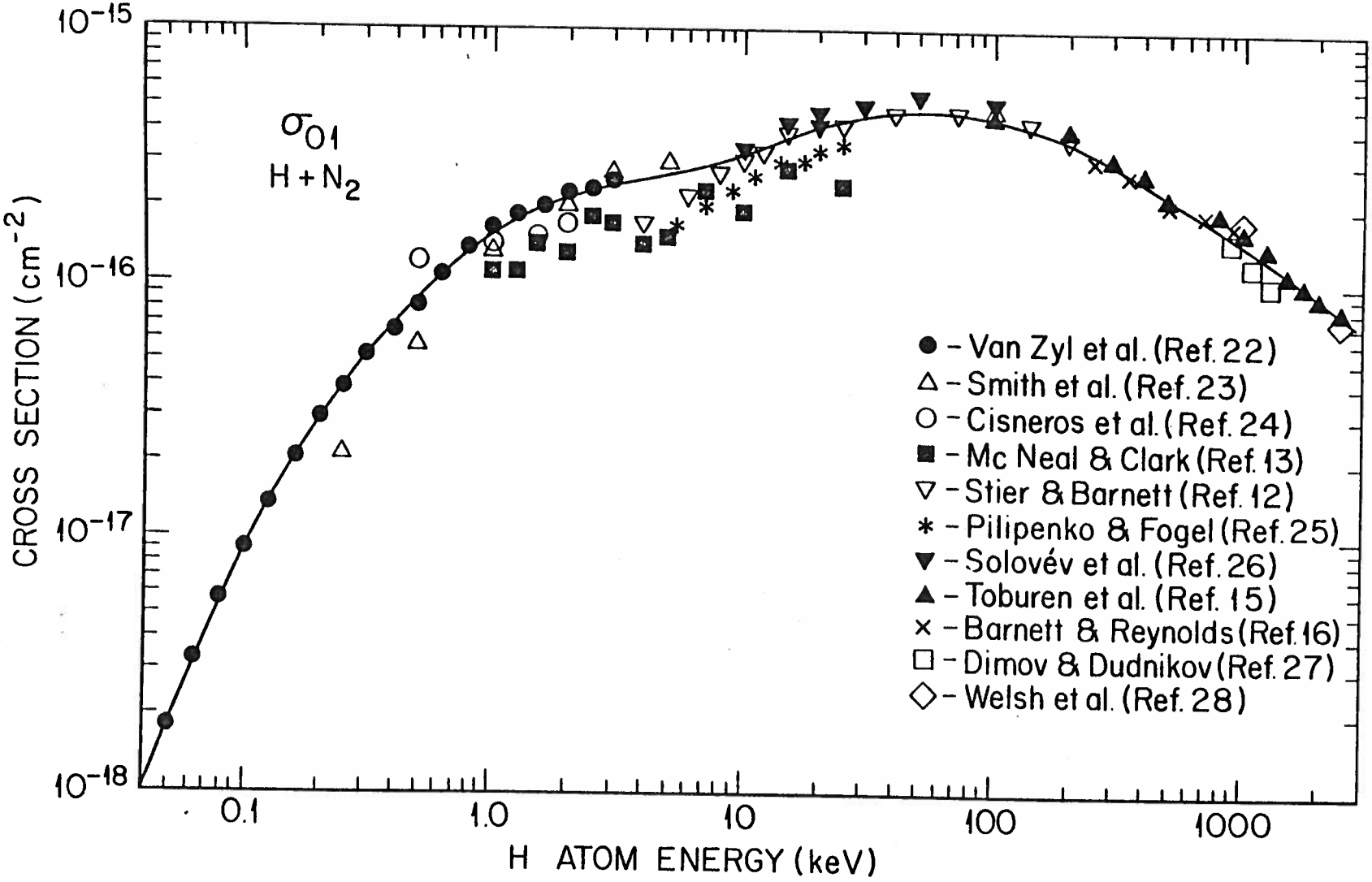

Figure 4. Ionization-stripping cross section for H atoms in N_2.

angularly scattered beyond their detector's collection capability.[29] The technique used by Van Zyl et al. should not be influenced by this problem.

While the energy dependence of the σ_{10} cross sections discussed in Section II are in basic agreement with the theory of such reactions, the ionization-stripping results cannot be explained so easily. For such inelastic collisions ($\Delta E \gtrsim 13.6$ eV, depending on the secondary electron energy), simple classical theory predicts that the cross sections should reach maxima in the 10 to 100 keV energy region. The σ_{01} cross section for N_2 targets does peak near 50 keV, but the broad "shoulder" on the cross section curve at lower energies is not predicted in this simple model. At the lower energies, the reaction probably proceeds via formation of a transient molecular complex. An even more pronounced low energy "shoulder" is found in the σ_{01} cross section for H + Ar collisions, and a possible mechanism to explain the observations has been suggested.[18] Even though such models are highly speculative, they do point to the need for including the quantum-mechanical details of such interactions in making cross section predictions.

b.) $H + O_2$

The results for the σ_{01} cross section for O_2 targets are presented in Fig. 5. In general, these data are rather similar to those for N_2 targets, and no further discussion is therefore required.

c.) H + O

There are no cross section data available for this important reaction at any energy. Thus, one must depend upon theoretical calculations or other forms of cross section estimates to obtain the desired information.

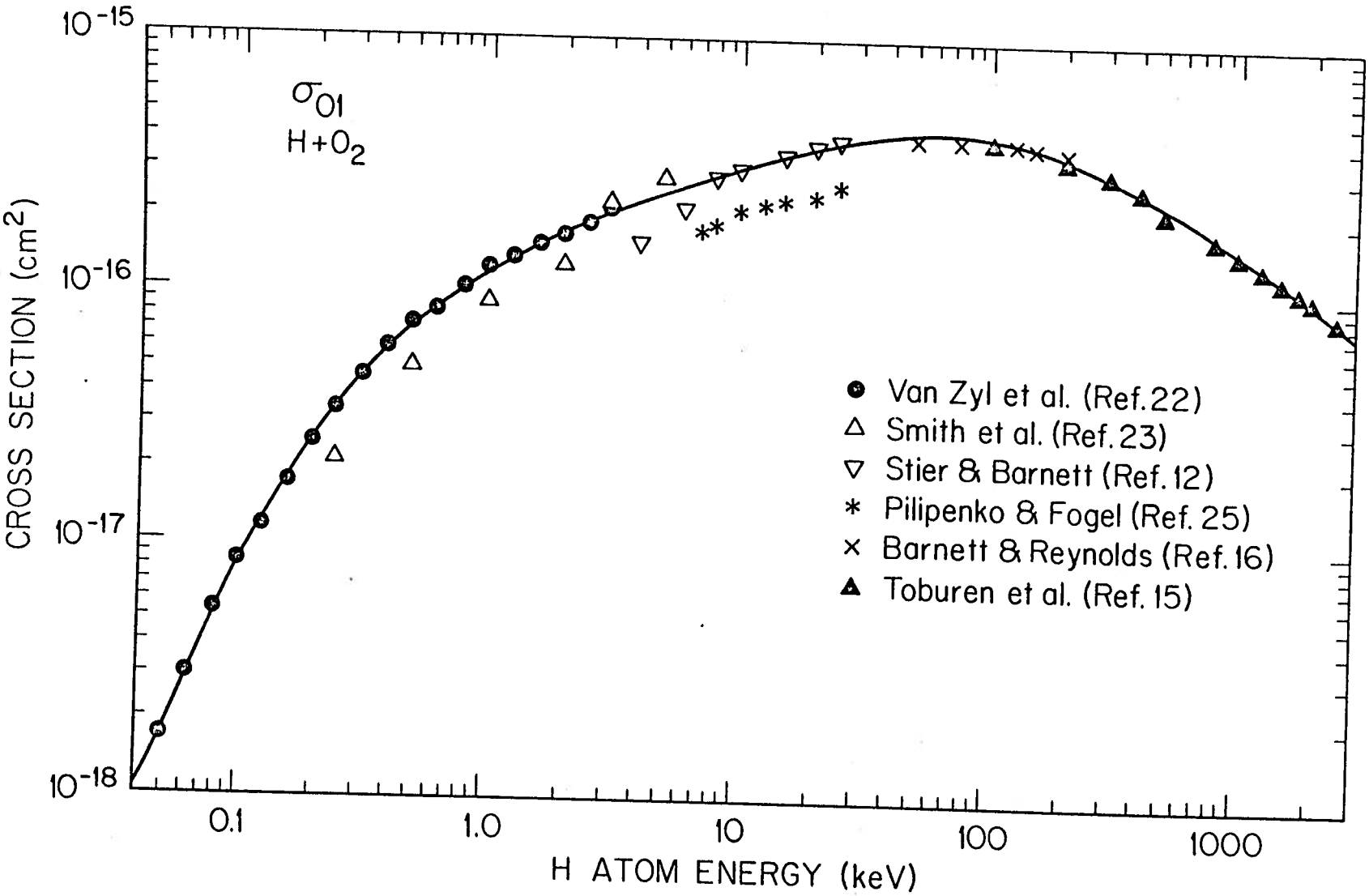

Figure 5. Ionization-stripping cross section for H atoms in O_2.

McNeal and Birely[2] have computed the σ_{01} cross section for atomic oxygen between 0.1 and 100 keV using a semiempirical technique developed by Green and McNeal.[30] Their results are compared with the measured ionization-stripping cross sections for N_2, O_2, and He targets in Fig. 6. Note first that the measured results for N_2 and O_2 are very similar, and even the data for He targets show a comparable energy dependence. (In fact, similar energy dependences are found for many such σ_{01} cross sections.[31]) As can be seen, the calculated results of McNeal and Birely do not fit this "pattern" very well. More specifically, it is difficult to believe that the σ_{01} cross section for O atoms should fall below that for He atoms, as the calculated results do between about 1 and 10 keV.

In the high energy region, where formation of a transient molecular complex is unimportant,[32] the effective ionization-stripping cross section should probably be roughly proportional to the "size" of the target species. Thus one might expect the σ_{01} cross section for atomic oxygen to be about 60% as large as that for O_2 (where I have averaged over the possible molecular orientations relative to the collision axis). If this were the case, however, it would follow that the cross section for H + Ar collisions should also be somewhat smaller than those for N_2 and O_2. To the contrary, experimental results show that the ionization-stripping cross section for Ar targets is essentially the same as those for these molecules.[31] In fact, the σ_{01} cross section for Ar is very similar to that for N_2 at all energies.[18,31]

It is apparent that neither rough comparisons nor semiempirical calculations are likely to yield an accurate σ_{01} cross section for H + O collisions. At 100 keV, where the calculation of McNeal and

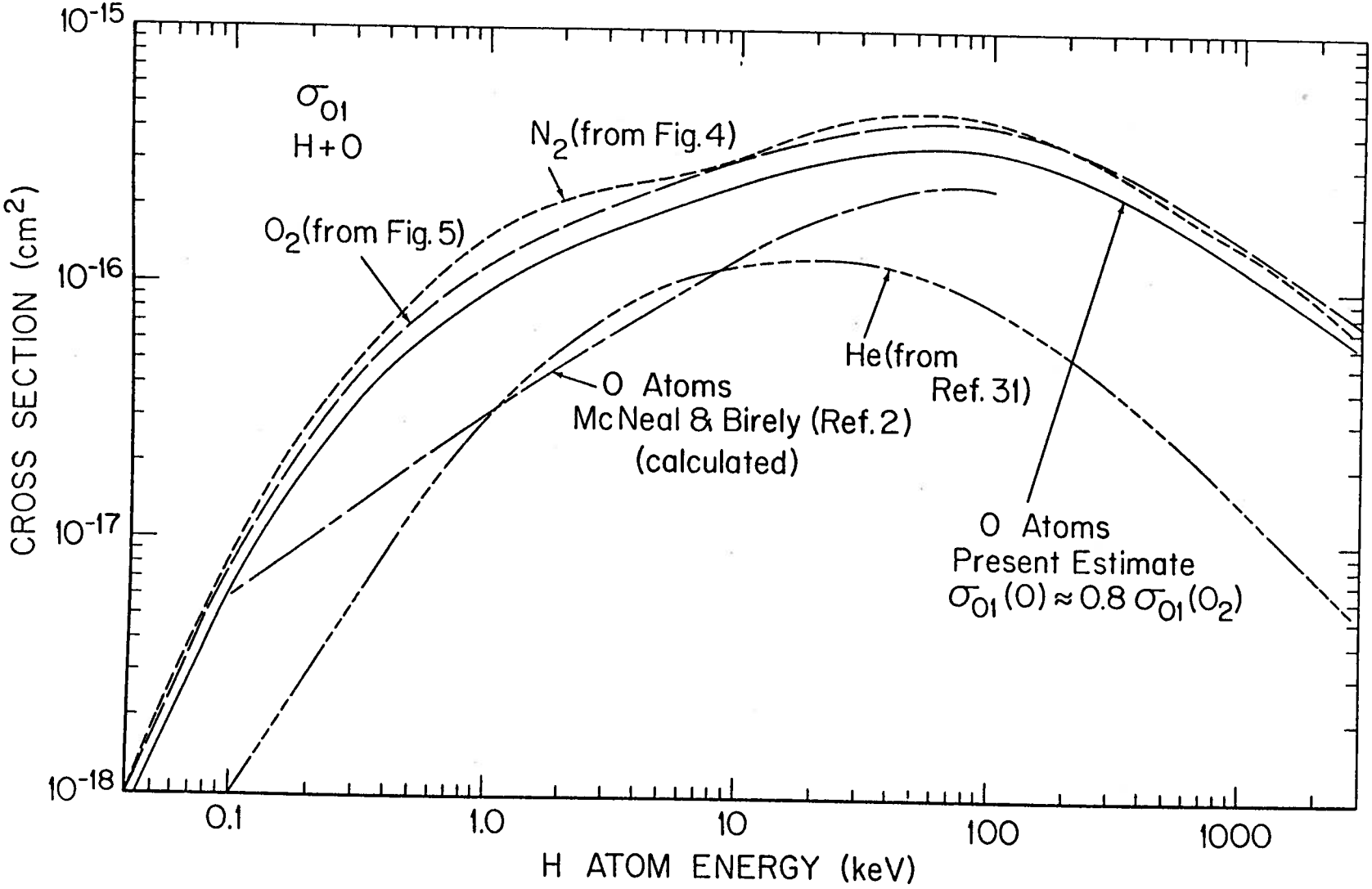

Figure 6. Ionization-stripping cross section for H atoms in O. The ionization-stripping cross sections for H + N_2, H + O_2, and H + He are shown for comparison.

Birely[2] is probably the most accurate, I will take a value approximately midway between their computed result and that obtained by averaging the cross sections for N_2, O_2, and Ar targets. This value turns out to be about 0.8 of that obtained for O_2 targets, and is probably a resonable estimate for energies above about 10 keV, with an uncertainty of perhaps ± 40%. As can be seen in Fig. 6, I have extended this estimate of the cross section magnitude into the lower energy region, an extension of dubious merit, but one I feel is more appropriate than using the results of the McNeal and Birely calculation. Fortunately, in this low energy region, the charge-exchange cross section σ_{10} for atomic oxygen is much larger than σ_{01}, resulting in a large value for the flux fraction F_0 which is thus rather insensitive to the exact σ_{01} magnitude. A more definitive determination of this σ_{01} cross section will have to wait for the results of future studies.

IV. CHARGE-STATE-EQUILIBRIUM FLUX FRACTIONS FOR N_2, O_2, AND O TARGETS

The values of the charge-state-equilibrium flux fractions F_0 and F_1 have been computed by Eq. 3 by using cross section values from the appropriate curves shown in Figs. 1 to 6. The results are plotted in Fig. 7 as a function of H^+/H energy. The values obtained for O_2 and O targets are essentially identical and only one curve is therefore shown for these species. Of course, the assumptions made for the magnitudes of σ_{10} and σ_{01} for atomic oxygen force this compliance.

As assessment of the uncertainties involved in these flux fractions is difficult. Above about 100 keV, where $\sigma_{10}/\sigma_{01} \ll 1$, the fraction F_1 is large and, when written as

$$F_1 = \frac{1}{1 + \sigma_{10}/\sigma_{01}}, \qquad (6)$$

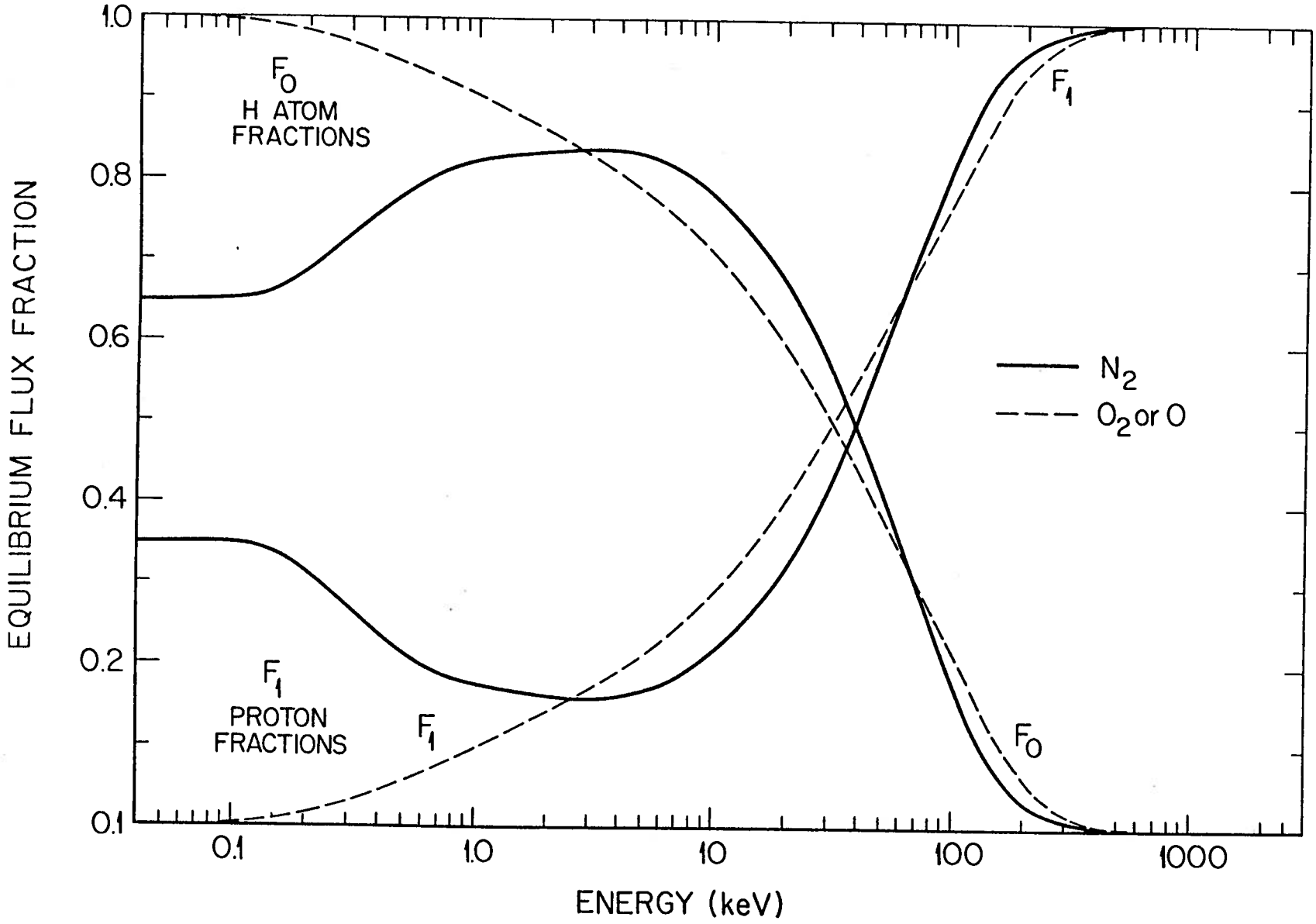

Figure 7. Charge-state-equilibrium flux fractions for N_2 and O_2 or O.

can be seen to be about unity, even when σ_{10}/σ_{01} is highly uncertain. A similar argument can be made for F_0 for O or O_2 targets below about 4 keV where $\sigma_{01}/\sigma_{10} << 1$. In the region between about 4 keV and 100 keV, a crude analysis of the accuracy of the cross section data used (for N_2 and O_2) gives uncertainties in the fractions of about $\pm$ 20% at 35 keV, where F_0 and F_1 are comparable. Where either fraction becomes larger, its uncertainty becomes smaller and, conversely, the smaller fraction exhibits an increasingly larger uncertainty. For the case of atomic oxygen, the uncertainties are probably about twice those for the molecular targets.

For the case of N_2 targets below a few hundred eV, the situation is not as clear. For example, if the σ_{10} value reported by Koopman[9] at 100 eV is used, the fraction F_0 increases form 0.65 to 0.87 (a 34% increase). Similarly, if the value for σ_{01} reported by Smith et al.[23] at 250 eV is adopted instead of that reported by Van Zyl et al.,[22] the fraction F_0 increases from 0.71 to 0.81 (a 14% increase) at that energy. Since both of these alternate data selections cause F_0 to increase at the lower energies, we may conclude that, even for N_2 targets, the bulk of the precipitating flux will be in the neutral H atom charge state.

V. APPLICATION TO THE HYDROGEN AURORA

Protons with 100 keV primary energy penetrate into the atmosphere to an altitude of about 100 km, depending on their pitch-angle distribution, while a 1 keV flux (as in the cusp aurora) would be stopped above 200 km. The composition of the atmosphere at these altitude levels is different as shown in Fig. 8, where the fractional concentratons of N_2, O_2, and O are shown as a function of altitude.[33] These data can be used to compute effective charge-state-equilibrium flux fractions for the

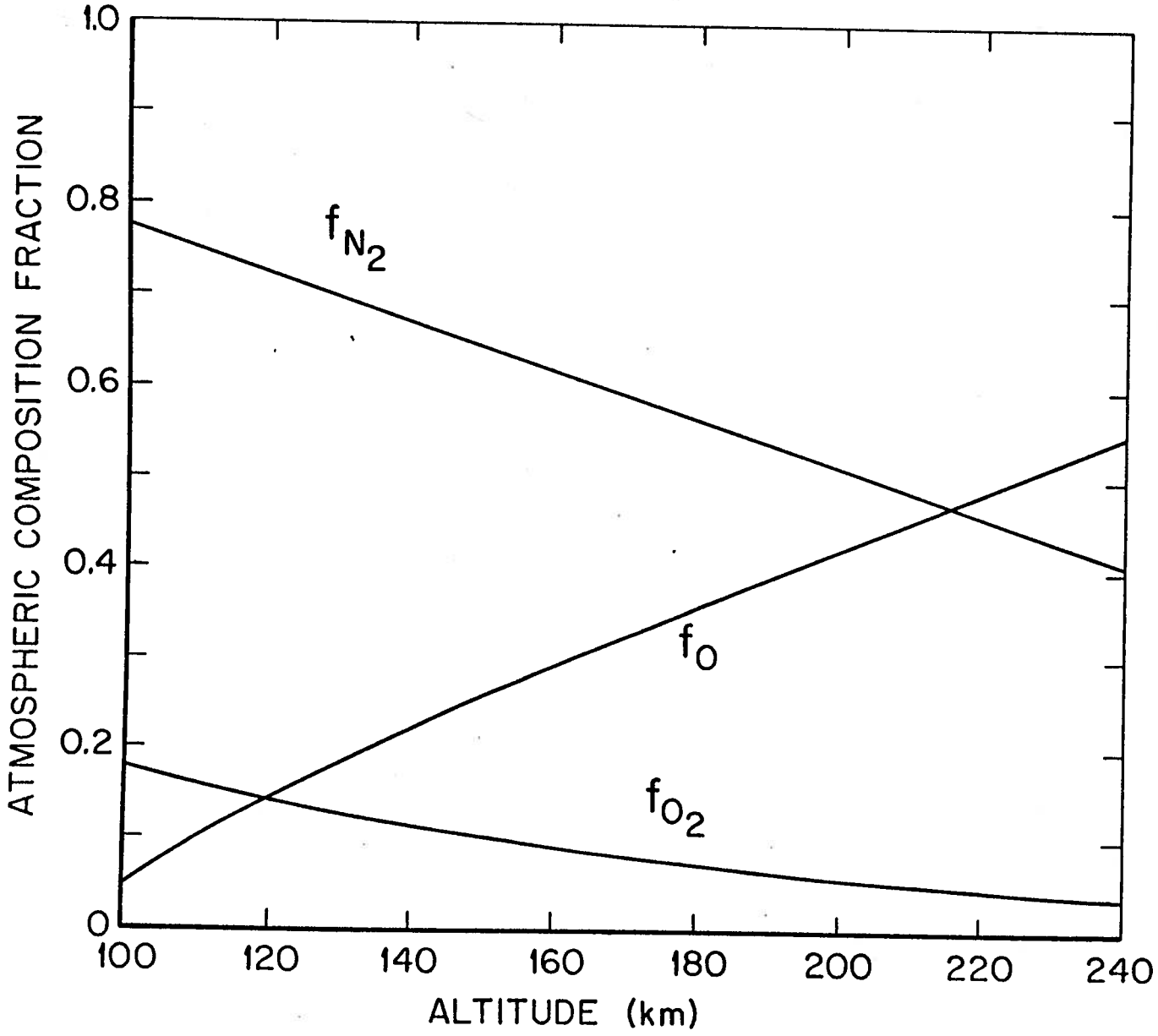

Figure 8. Relative atmospheric composition versus altitude.

atmospheric medium from the relationship

$$F_1^{eff} = f_{N_2} F_1(N_2) + f_{O_2} F_1(O_2) + f_O F_1(O) \qquad (7)$$

and its counterpart for F_0^{eff}, where f_{N_2}, f_{O_2}, and f_O are the composition fractions shown in Fig. 8.

Computations of F_1^{eff} and F_0^{eff} as a function of altitude yield families of curves basically similar in shape to those shown in Fig. 7. At energies below 2 keV, these flux fractions assume different values at different altitudes, but above 2 keV, they are altitude independent to within an uncertainty far smaller than the uncertainties in the individual F_1 and F_0 values for the various targets. The values of F_1^{eff} and F_0^{eff} shown in Fig. 9 may therefore be used for working flux fractions in the atmosphere. The appropriate flux fractions at other altitudes can be obtained by interpolation of the data presented.

VI. SUMMARY

The charge-state-equilibrium flux fractions for a mixed H^+/H flux moving through the terrestrial atmosphere have been computed as a function of energy and altitude. The results show that below about 35 keV, more than half of the precipitating flux is in the neutral H atom charge state, this fraction increasing to about 80% at energies below 10 keV.

The results presented here are not appreciably different from the older data presented by Allison[6] for energies above a few keV for N_2 and O_2 targets. The flux fractions for these atmospheric constituents are now available for the entire range of energies of interest in the hydrogen aurora.

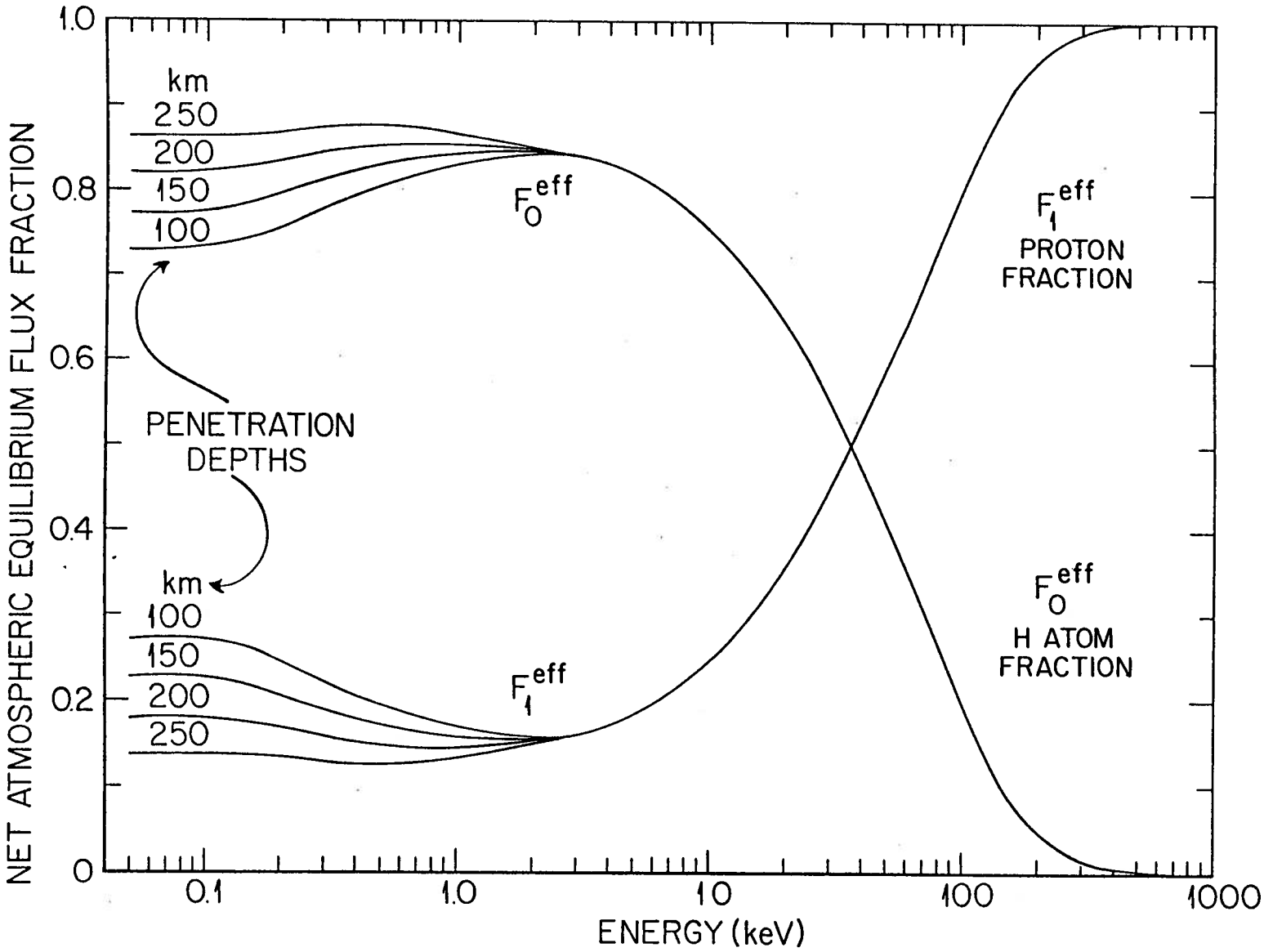

Figure 9. Effective atmospheric charge-state-equilibrium flux fractions.

In contrast, the results presented here for atomic oxygen are at variance with the predictions of McNeal and Birely.[2] Further experimental or theoretical work is clearly needed for this important atmospheric target before more definitive flux fractions can be obtained.

REFERENCES AND FOOTNOTES

1.) L. Vegard, Nature 144, 1089 (1939).

2.) R. J. McNeal and J. H. Birely, Rev. Geophys. Space Phys. 11, 633 (1973).

3.) R. H. Eather, Rev. Geophys. Space Phys. 5, 207 (1967).

4.) See, for example, V. A. Gladyshev, M. V. Jorjio, F. K. Shuishaya, J. Crasnier, and J. A. Sauvaud, Annls. Geophys. 30, 301 (1974).

5.) Some small fraction of the incident protons will also be converted to negative hydrogen ions (H^-). However, the ionization-stripping cross sections for such ions, σ_{-10}, are large and result in the rapid conversion of the H^- ions back to neutral H atoms. Thus the role of H^- ions in the production of most auroral features is probably small and they will be ignored here.

6.) S. K. Allison, Rev. Mod. Phys. 30, 1137 (1958).

7.) E. Gustafsson and E. Lindholm, Arkiv. Fysik. 18, 219 (1960).

8.) G. Monnom, M. Eliot, J. Guidini, and F. P. G. Valckx, C. R. Acad. Sc. Paris 281, 425 (1975).

9.) D. W. Koopman, Phys. Rev. 166, 57 (1968).

10.) H. B. Gilbody and J. B. Hasted, Proc. Roy. Soc. (London) A238, 334 (1956).

11.) Yu. S. Gordeev and M. N. Panov, Sov. Phys.-Tech. Phys. 9, 656 (1964).

12.) P. M. Stier and C. F. Barnett, Phys. Rev. 103, 896 (1956).

13.) R. J. McNeal and D. C. Clark, J. Geophys. Res. 74, 5065 (1969).

14.) F. J. deHeer, J. Schutten, and H. Moustafa, Physica 32, 1766 (1966).

15.) L. H. Toburen, M. Y. Nakai, and R. C. Langley, Phys. Rev. 171, 114 (1968).

16.) C. F. Barnett and H. K. Reynolds, Phys. Rev. 109, 355 (1958).

17.) U. Schryber, Helvetia Physica ACTA 39, 562 (1966).

18.) B. Van Zyl, T. Q. Le, H. Neumann, and R. C. Amme, Phys. Rev. A 15, 1871 (1977). This paper reports work with a similar type collision cell geometry where such scattering was found to have an E^{-1} energy dependence.

19.) D. Rapp and W. E. Francis, J. Chem. Phys. 37, 2631 (1962).

20.) R. F. Stebbings, A. C. H. Smith, and H. Ehrhardt, J. Geophys. Res. 69, 2349 (1964).

21.) D. R. Bates and R. McCarrol, Proc. Roy. Soc. (London) A245, 175 (1958).

22.) B. Van Zyl, H. Neumann, T. Q. Le, and R. C. Amme, Phys. Rev. A 18, 506 (1978).

23.) K. A. Smith, M. D. Duncan M. W. Geis, and R. D. Rundel, J. Geophys. Res. 81, 2231 (1976).

24.) C. Cisneros, I. Alvarez, C. F. Barnett, and J. A. Ray, Phys. Rev. A 14, 84 (1976).

25.) D. V. Pilipenko and Ya. M. Fogel, Sov. Phys. JETP 15, 646 (1962).

26.) E. S. Solov'ev, R. N. Il'in, V. A. Oparin, and N. V. Fedorenko, Sov. Phys. JETP 15, 459 (1962).

27.) G. I. Dimov and V. G. Dudnikov, Sov. Phys.-Tech. Phys. 11, 919 (1967).

28.) L. M. Welsh, K. H. Berkner, S. N. Kaplan, and R. V. Pyle, Phys. Rev. 158, 85 (1967).

29.) For the case of H + H_2 collisions, where the light target results in substantially less large-angle-scattering of the product protons, the results of Van Zyl et al. (to be published) and Smith et al. (Ref. 23) are in excellent agreement. A slight divergence begins to appear for H + He collisions, and seems to increase with the target mass for the "heavy" molecules of interest here. This type of behavior seems to suggest that angular scattering lies at the root of this discrepancy.

30.) A. E. S. Green and R. J. McNeal, J. Geophys. Res. 76, 133 (1971).

31.) H. Tawara and A. Russek, Rev. Mod. Phys. 45, 178 (1973). The data for He below 3 keV are from unpublished work by Van Zyl et al. (to be published).

32.) At collision velocities well above 10^8 cm/sec., the orbital electrons of the hydrogen atom and the target atom have insufficient time to adjust to one another as the collision proceeds.

33.) U. S. Standard Atmosphere. Spring/fall Model. Exospheric Temperature = 1100°K.